ChemComm

Accepted Manuscript

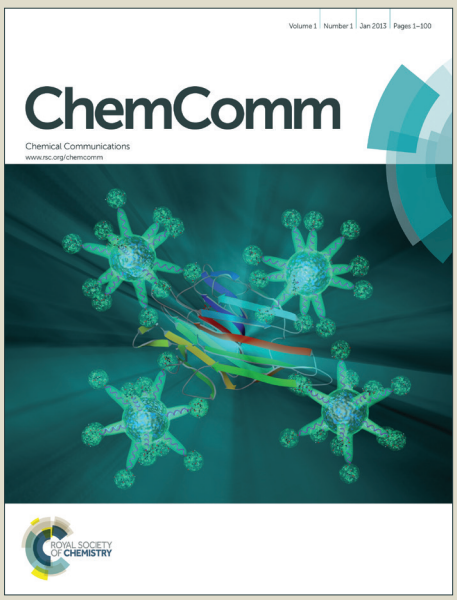

ROYAL SOCIETY OF CHEMISTRY

www.rsc.org/chemcomm

Journal Name

RSCPublishing

COMMUNICATION

Single-molecule dynamics of site-specific labeled transforming growth factor type II receptors on living cells

Cite this: DOI: 10.1039/x0xx00000x

Received 00th January 2012,
Accepted 00th January 2012

DOI: 10.1039/x0xx00000x

www.rsc.org/chemcomm

Ming Cheng,[a] Wei Zhang,[a] Jinghe Yuan,[a] Wangxi Luo,[a] Nan Li,[a] Shixian Lin,[b] Yi Yang,[b] Xiaohong Fang*[a] and Peng R. Chen*[b]

We achieved single-molecule imaging and tracking of the transforming growth factor type II receptor (TβRII) that was labeled by an organic dye via a genetically encoded unnatural amino acid (UAA) and the copper-free click chemistry. The stoichiometry, mobility and dimerization kinetics of individual TβRII molecules were determined.

Fluorescent labeling and imaging of proteins is becoming an important technique for the study of biological processes at cellular and subcellular levels. Although fluorescent proteins (FPs) are widely used reporters both *in vitro* and *in vivo*, they have some drawbacks including bulky size, poor photostability, as well as the largely restricted labeling sites at the N- or C- terminus of a protein of interest (POI).[1] In recent years, the combination of bioorthogonal reactions with the genetic-code expansion strategy has been developed as a valuable alternative approach for protein labeling.[2] Recent work have demonstrated that UAAs bearing a bioorthogonal group can be site-specifically incorporated into a POI via the genetic code expansion strategy, which can be subsequently conjugated with a small-molecule fluorophore. This approach features in high specificity and low perturbation during the labeling process, allowing the probing of the structure and function of POI in living bacteria, mammalian cells, and even in animals.[3] Moreover, the conjugation of proteins with photo-stable organic dyes at an accurate 1:1 ratio offers a great advantage for monitoring single protein molecule. Recently, genetically encoded UAAs were developed for site-specific labeling of a POI, allowing the in vitro single-molecule fluorescence resonance energy transfer (smFRET) analysis of protein conformational and structural changes in solution.[4] Nevertheless, applying this site-specific labeling strategy for single-molecule study is still in its infancy. Single-molecule imaging of a UAA incorporated nicotinic receptor was just achieved by Pantoja *et al*.[5] In their study, a UAA was firstly conjugated with a fluorescent dye and the resulting fUAA was injected into Xenopus oocytes, followed by the injection of the chemically modified transfer RNAs (tRNAs) and associated aminoacyl-tRNA synthetase. This requires relatively complicated microinjection operations and the expression efficiency of the fUAA-incorporated receptor is low. Single-molecule dynamic study of site-specifically labeled proteins in living mammalian cells, which requires the in-situ chemical reaction is unachieved and remains challenging.

In this study, we reported the live-cell single-molecule imaging and tracking of fluorescently labeled membrane protein TβRII that was site-specifically incorporated with an azide-bearing UAA handle. TβRII is a cell surface receptor protein that plays important roles in diverse physiological and pathological processes. Our previous single-molecule microscopic study using GFP-tagged TβRII revealed the ligand induced dimerization of this critical surface receptor during TGF-β signaling.[6] However, the fused bulky GFP molecule may interfere with the structure and function, particularly the monomer-dimer interconversion equilibrium of TβRII. Herein, we labeled TβRII with a small dye molecule via the azido-UAA in this study. Single-molecule fluorescence imaging of the labeled TβRII allowed us to determine not only stoichiometry, but also mobility and dimerization kinetics of individual TβRII molecules within their native cellular environment.

We started by constructing the TβRII variant bearing an in-frame amber codon in its extracellular domain as well as a C-terminal reporter gene (eGFP or HA) for verification of the UAA insertion efficiency. The extracellular residues Asn40, Lys82 and Glu91 which were all located away from the ligand-binding sites were chosen as the UAA-insertion sites on TβRII to minimize the influence on receptor activation (Figure 1A). The pyrrolysine (Pyl)-based genetic-code expansion system was employed.[7] We have previously developed an azide-bearing, cyclic-Pyl analogue ACPK (Figure 1B) that can be site-specifically incorporated into a POI by a mutant Pyl tRNA synthetase, termed ACPK-RS, and its cognitive $tRNA^{Pyl}_{CUA}$ with high efficiency and fidelity.[3b, 8] The expression level of proteins bearing the genetically encoded ACPK is about two-fold higher than that of a linear azido-Pyl analogue recognized by the wild-type PylRS- $tRNA^{Pyl}_{CUA}$ pair. [9]

To examine whether our ACPK-bearing TβRII variants affected the TGF-β signaling, the activities of all three TβRII-ACPK variants were inspected by a dual luciferase assay (Figure 1C). The CAGA12-luciferase reporter is commonly

used to detect the TGF-β downstream Smads proteins after TβRII activation. Both TβRII-40ACPK and TβRII-91ACPK variants (containing HA and GFP tag), but not the TβRII-82ACPK variant were found to be fully functional in activating the expression of TGF-β-responsive reporter in the presence of TGF-β1, indicating that TβRII carrying an ACPK at residue 40 or 91 possess normal physiological functions. Notably, whereas no statistic difference was observed between HA-TβRII-ACPK and HA-TβRII ($p>0.05$, t-test), the relative activity of TβRII-GFP and TβRII-ACPK-GFP showed significant differences when compared with HA-TβRII ($p<0.01$, t-test). Since it is known that the HA tag has negligible effects on TβRII, these results indicated that, in contrast to the C-terminal fusion of GFP, the site-specific incorporation of ACPK at residues 40 and 91 on TβRII resulted in little effect on its downstream signaling.

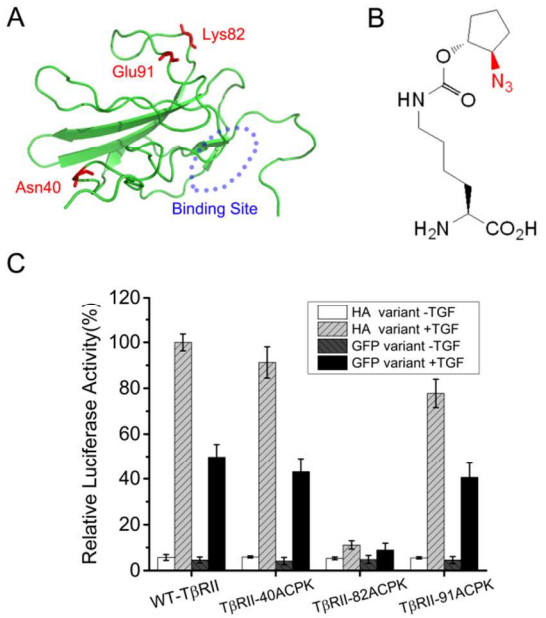

Figure 1. Site-specific introduction of the azido functionality into the extracellular domain of TβRII. (A) Structure of the extracellular domain of TβRII with the UAA insertion sites labeled in red. (B) Structure of the azide-bearing unnatural amino acid ACPK (Nε-(((1R, 2R)-2-azidocyclopentyl) oxy) carbonyl)-L-lysine) (C) The activity of the ACPK-bearing TβRII variants examined by dual luciferase assay. The results were normalized by that of wide-type TβRII (WT-TβRII).

After confirming the effectiveness of TβRII-ACPK variants, we examined the expression of TβRII-ACPK-GFP on the cell membrane.[10] We observed fluorescent spots of TβRII-ACPK-GFP on HeLa membranes only after ACPK incubation (Figure S1A, B). The results confirmed the successful insertion of ACPK into TβRII. We also checked the transfection efficiency of three TβRII-ACPK variants (Figure S1C). Considering its highest signaling activity and expression level, we chose the TβRII-40ACPK variant for all the following experiments. Because ACPK did not possess the fluorescence signal itself, and HA tag could be only labeled in fixed cells, we fluorescently labeled TβRII through the azido-group on ACPK by Cu-free click chemistry to avoid the possible cytotoxicity of Cu (I) ions for live cell imaging. The strain-promoted azide–alkyne cycloaddition (SPAAC) with a Dibenzocyclooctyne (DBCO)-conjugated fluorophore was used as the labeling reagent. Recent reports showed that cyclooctyne might react with thiols in proteins and thus produce a high background during intracellular protein labeling.[11] However, cell surface labeling through the SPAAC reaction has been widely adopted with less concerns, particularly for labeling of surface glycans and glycosolated proteins.[12] Here we used DBCO-conjugated Fluor 545 (DBCO545, Figure S1D) to couple ACPK via SPAAC because of its high photo-stability, quantum yield, and pH stability.[13] To confirm DBCO545 was selectively linked to ACPK, we performed a colocalization experiment with cells transfected by HA-TβRII-40ACPK or HA-TβRII. When cells were stained with both DBCO545 and anti-HA conjugated Alexa Fluor 488 (HA488), only those transfected with HA-TβRII-40ACPK showed an obvious colocalization (Figure S1E, F). These results demonstrated that the azide-bearing TβRII was labeled by the organic dye with excellent specificity. The dye labeled TβRII also had similar signalling ability as the wild-type TβRII (Figure S2).

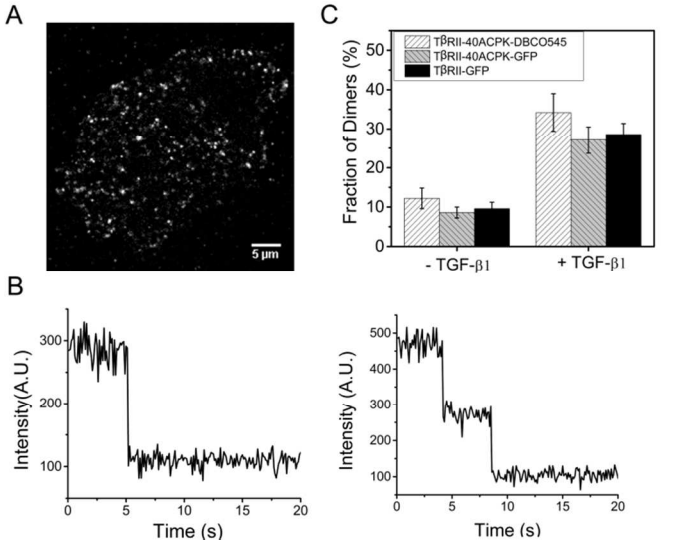

Figure 2. Ligand induced TβRII dimerization. (A) Typical TIRF image of TβRII-40ACPK-DBCO545 molecules in living HeLa cells after background subtraction. (B) Two representative time courses of the fluorescent spots showed one-step bleaching or two-steps bleaching. (C) Dimer fractions of TβRII-40ACPK-DBCO545, TβRII-40ACPK-GFP and TβRII-GFP on cell membrane before and after TGF-β1 treatment. Error bars represent SEM.

In our previous work, we have revealed that GFP tagged TGF-β receptors follow the new ligand-induced receptor dimerization model for activation. [6] However, tagging a large GFP (27 kDa) molecule to TβRII (~80 kDa) raised the concern on the interference of GFP. In this work, we chose the TβRII-40ACPK variant labeled with small-molecule DBCO545, to investigate the stoichiometry of TβRII receptors. TβRII-40ACPK-DBCO545 molecules were imaged at low density (~ 0.08-0.25 copies / μm^2) by TIRFM. As shown in a typical image of a HeLa cell (Figure 2A), TβRII molecules could be

distinguished as well-dispersed diffraction-limited fluorescent spots whose PSF were fitted well with Gaussian function before and after TGF-β1 stimulation. They maintained fluorescent signals for a few seconds and then suddenly disappeared, indicating single-molecule imaging.

With the single-molecule imaging of TβRII-40ACPK-DBCO545, we firstly investigated the fluorescence intensity distribution of individual TβRII spots on cell membrane before TGF-β1 stimulation. The histogram of the fluorescent intensities was fitted by the sum of two Gaussian functions (Figure S3). The peak intensity of the large population was approximate to that of single dispersed DBCO545 molecules on coverslips, suggesting the majority of spots represented monomeric TRβII molecules. Further analysis showed 10.8% of TβRII-40ACPK-DBCO545 was dimer and the dimer population increased to 42.9% after ligand stimulation. To confirm the stoichiometry change of TβRII, the photobleaching step analysis was performed in fixed HeLa cells.[14] Most TβRII-40ACPK-DBCO545 fluorescent spots showed clearly one-step or two-step photobleaching characteristics, indicating monomers or dimers (Figure 2B). The dimers population increased markedly with the increased receptor density after 200 pM ligand treatment (Figure 2C). These results were in consisted with that from fluorescence distribution, and suggested that monomeric TβRII underwent dimerization after ligand stimulation. Cells expressing TRβII-40ACPK-GFP and TβRII-GFP were also investigated and the same tendency was found (Figure 2C). Similar results were obtained using endogenous TβRII deficient MCF-7 cells. (Figure S4)

We further tracked the lateral diffusion of individual TβRII-40ACPK-DBCO545 molecules on living cell membrane. During the tracking, the dynamic change of TβRII between the two states of monomer and dimer was discovered (Supporting Movie 1). As shown in Figure 3, TβRII molecules diffused on the membrane and frequently displayed colocalization and codiffusion. The changes in fluorescence intensity were consistent with reversible dimer formation.

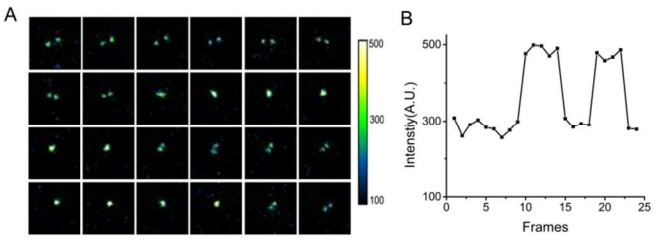

Figure 3. A) Illustration of two TβRII-40ACPK-DBCO545 receptors that associated and separated dynamically within 24 sequential frames (50 ms/frame, 30 * 30 pixels) on the surface of a living HeLa cell with a pseudo color look-up table. B) Intensity trajectory of one individual TβRII-40ACPK-DBCO545 molecule (left spot in the first image of A) that exhibited reversible intensity changes.

The histogram of dimer duration time (~1000 individual dimers) could be fitted with a single exponential function to determine the dimer lifetime, which was 253 ms (Figure 4A). This value can be differentiated from both the monomer incidental colocalization time (less than 100 ms which was obtained by checking the colocalization of two unrelated molecules, EGFR and TβRII) and the photobleaching time of DBCO545 (4.1 s). The determined lifetime of TβRII dimer is in the same magnitude order as the reported membrane receptors, such as M1 muscarinic receptor and N-formyl peptide receptor.[15]

It is noted that if we need to follow the dynamic change of individual molecules, the advantages of organic dyes in photostability and size were obvious. DBCO545 labeled TβRII showed a longer photobleaching time (4.1s) than that of GFP (2.5 s) and a higher signal / noise ratio under the same imaging conditions, facilitating the observation of multiple monomer-dimer dynamic transitions to obtain reliable dimer lifetime. Moreover, considering the lower diffusion rate and lower signaling activity of TβRII-GFP, the monomer-dimer equilibrium of DBCO545 labeled TβRII would be more physiologically relevant.

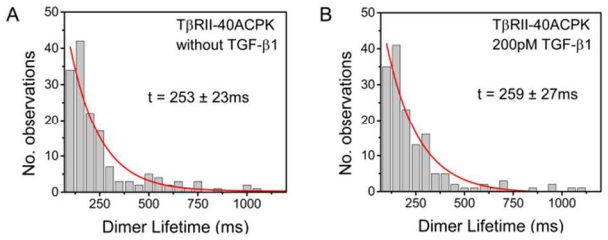

Figure 4. Histogram of the lifetimes of TβRII-40ACPK receptor dimers obtained from trajectories collected in 50 ms bins before (A) , after (B) 200 pM ligand stimulation. The solid line is a monoexponential fit for a mean lifetime.

We then measured the TβRII dimer duration time after ligand treatment. Surprisingly, the dimers duration time after 200 pM TGF-β1 stimulation showed no statistical discrepancy with the untreated group ($p<0.05$，t-test) (Figure 4C). Higher TGF-β1 concentrations such as 600 pM and 2000 pM were investigated by the same method but the dimer duration time was still unchanged. These results indicated that the presence of TGF-β1 did not influence the TβRII homodimer lifetime. This result was also confirmed by the measuring dimer lifetime according to their diffusion rate change before and after ligand treatment. The averaged dissociation rate constants (kd) of TβRII dimer were calculated as 3.95 ± 0.33 s^{-1} at the resting state and 3.86 ± 0.36 s^{-1} after 200 pM ligand stimulation from three experiments.

The above results provided the first evidence on the dynamic monomer-dimer equilibrium of TβRII molecules on cell membrane even before ligand stimulation, and discovered this equilibrium is ligand-independent. Since receptor oligomerization plays a critical role in the control of cell signal transduction, quantitative evaluations on the receptor stoichiometry change would greatly advance our understanding of the time-dependent changes of cell signaling intensity and the fundamental mechanism of signal transduction.[15a, 16] For most of growth factor receptors with such an activation model, it has been assumed that the ligand could stabilize the dimer, thus the increased dimer lifetime contributes to signal

transduction.[17] However, our results here on the dynamic monomer-dimer equilibrium of TβRII did not support this general assumption. Although more TβRII dimers were found after ligand stimulation, it was not caused by the dimer lifetime enhancement. A recent single-molecule study of EGFR found the similar evidence that EGF did not stabilize EGFR dimer. We have noticed that after ligand treatment, the receptor density on the cell membrane increased (Figure S5). This may be the reason for the increased TβRII dimer population, since we have found the population of TβRII dimers was strongly related to its density. [10]

In conclusion, we have site-specifically incorporated the azide-bearing ACPK amino acid into TβRII to achieve single-molecule fluorescence imaging of TβRII molecules on live cell surface. Results obtained from this precisely labeled TβRII provided valid evidence that confirmed our recently proposed new activation model for TGF-β receptors with GFP-fused TβRII. More importantly, our work revealed new information on the dynamics of TβRII monomer-dimer equilibrium which could lead to a better understanding of TGF-β signaling processes. Applying this bioorthogonal and site-specific protein labeling strategy to single-molecule imaging offers a great potential for the functional and dynamics study of diverse surface proteins on living cells.

Notes and references

[a] Beijing National Laboratory for Molecular Sciences, Institute of Chemistry, Key Laboratory of Molecular Nanostructures and Nanotechnology, Chinese Academy of Sciences, Beijing 100190, P. R. China

[b] Beijing National Laboratory for Molecular Sciences, Synthetic and Functional Biomolecule Centre, Department of Chemical Biology, Peking University, Beijing 100871, P. R. China Address here.

† This work was supported by National Basic Research Program of China (2013CB933701 to X.F., and 2010CB912302 to P.R.C.), NSFC (No. 91213305, 21121063to X.F., and 21225206 to P.R.C.).

Electronic Supplementary Information (ESI) available: [details of any supplementary information available should be included here]. See DOI: 10.1039/c000000x/

1. N. C. Shaner, P. A. Steinbach and R. Y. Tsien, *Nat. Methods*, 2005, **2**, 905-909.
2. (a) D. A. Dougherty, *Curr. Opin. Chem. Bio.*, 2000, **4**, 645-652; (b) A. J. de Graaf, M. Kooijman, W. E. Hennink and E. Mastrobattista, *Bioconjugate. Chem.*, 2009, **20**, 1281-1295; (c) L. Rong, L.-H. Liu, S. Chen, H. Cheng, C.-S. Chen, Z.-Y. Li, S.-Y. Qin and X.-Z. Zhang, *Chem. Commun.*, 2013, **50**, 667-669.
3. (a) Z. Hao, S. Hong, X. Chen and P. R. Chen, *Acc. Chem. Res.*, 2011, **44**, 742-751; (b) S. Lin, Z. Zhang, H. Xu, L. Li, S. Chen, J. Li, Z. Hao and P. R. Chen, *J. Am. Chem. Soc.*, 2011, **133**, 20581-20587. (c) F. Li, H. Zhang, Y. Sun, Y. Pan, J. Zhou and J. Wang, *Angew. Chem.*, 2013, **125**, 9882-9886.
4. (a) J. Kim, M.-H. Seo, S. Lee, K. Cho, A. Yang, K. Woo, H.-S. Kim and H.-S. Park, *Anal. Chem.*, 2013, **85**, 1468-1474; (b) S. Milles, S. Tyagi, N. Banterle, C. Koehler, V. VanDelinder, T. Plass, A. P. Neal and E. A. Lemke, *J. Am. Chem. Soc.*, 2012, **134**, 5187-5195;
5. R. Pantoja, E. A. Rodriguez, M. I. Dibas, D. A. Dougherty and H. A. Lester, *Biophys. J.*, 2009, **96**, 226-237.
6. W. Zhang, Y. Jiang, Q. Wang, X. Ma, Z. Xiao, W. Zuo, X. Fang and Y. G. Chen, *Proc. Natl. Acad. Sci.*, 2009, **106**, 15679-15683.
7. (a) J. Xie and P. G. Schultz, *Nat. Rev. Mol. Cel. Bio.*, 2006, **7**, 775-782; (b) S. Greiss and J. W. Chin, *J. Am. Chem. Soc.*, 2011, **133**, 14196-14199.
8. Z. Hao, Y. Song, S. Lin, M. Yang, Y. Liang, J. Wang and P. R. Chen, *Chem. Commun.*, 2011, **47**, 4502-4504.
9. D. P. Nguyen, H. Lusic, H. Neumann, P. B. Kapadnis, A. Deiters and J. W. Chin, *J. Am. Chem. Soc.*, 2009, **131**, 8720-8721.
10. W. Zhang, J. Yuan, Y. Yang, L. Xu, Q. Wang, W. Zuo, X. Fang and Y.-G. Chen, *Cell Res*, 2010, **20**, 1216-1223.
11. P. V. Chang, J. A. Prescher, E. M. Sletten, J. M. Baskin, I. A. Miller, N. J. Agard, A. Lo and C. R. Bertozzi, *Proc. Natl. Acad. Sci.*, 2010, **107**, 1821-1826.
12. S. T. Laughlin, J. M. Baskin, S. L. Amacher and C. R. Bertozzi, *Science*, 2008, **320**, 664-667.
13. N. J. Agard, J. A. Prescher and C. R. Bertozzi, *J. Am. Chem. Soc.*, 2004, **126**, 15046-15047.
14. (a) M. H. Ulbrich and E. Y. Isacoff, *Nat. Methods*, 2007, **4**, 319-321; (b) W. Ji, P. Xu, Z. Li, J. Lu, L. Liu, Y. Zhan, Y. Chen, B. Hille, T. Xu and L. Chen, *Proc. Natl. Acad. Sci.*, 2008, **105**, 13668-13673.
15. (a) R. S. Kasai, K. G. N. Suzuki, E. R. Prossnitz, I. Koyama-Honda, C. Nakada, T. K. Fujiwara and A. Kusumi, *J. Cell. Bio.*, 2011, **192**, 463-480; (b) J. A. Hern, A. H. Baig, G. I. Mashanov, B. Birdsall, J. E. T. Corrie, S. Lazareno, J. E. Molloy and N. J. M. Birdsall, *Proc. Natl. Acad. Sci.*, 2010, **107**, 2693-2698.
16. (a) A. H. Clayton, F. Walker, S. G. Orchard, C. Henderson, D. Fuchs, J. Rothacker, E. C. Nice and A. W. Burgess, *J. Bio. Chem.*, 2005, **280**, 30392-30399; (b) P. Mehta, G. Jovanovic, T. Lenn, A. Bruckbauer, C. Engl, L. Ying and M. Buck, *Nat. Commun.*, 2013, **4**.
17. N. Kunishima, Y. Shimada, Y. Tsuji, T. Sato, M. Yamamoto, T. Kumasaka, S. Nakanishi, H. Jingami and K. Morikawa, *Nature*, 2000, **407**, 971-977.

